

Ising Spin Glasses and Renormalization Group Theory : the Binder cumulant

P. H. Lundow¹ and I. A. Campbell²

¹*Department of Mathematics and Mathematical Statistics, Umeå University, SE-901 87 Umeå, Sweden*

²*Laboratoire Charles Coulomb (L2C), UMR 5221 CNRS-Université de Montpellier, Montpellier, F-France.*

Numerical data on scaling of the normalized Binder cumulant and the normalized correlation length are shown for the Thermodynamic limit regime, first for canonical Ising ferromagnet models and then for a range of Ising spin glass models. A fundamental Renormalization Group Theory rule linking the critical exponents for the two observables is well obeyed in the Ising models, but not for the Ising spin glasses in dimensions three and four. We conclude that there is a violation of a standard Josephson hyperscaling rule in Ising spin glasses.

PACS numbers: 75.50.Lk, 75.40.Mg, 05.50.+q

I. INTRODUCTION

The consequences of the Renormalization Group Theory (RGT) approach have been studied in exquisite detail in numerous regular physical models, typified by the canonical near neighbor interaction ferromagnetic Ising model. It has been tacitly assumed that Edwards-Anderson Ising Spin Glasses (ISGs), where the interactions are random, follow the same basic scaling and Universality rules as the regular models.

The Binder cumulant [1] is an important observable which has been almost exclusively exploited numerically for its scaling properties as a dimensionless observable very close to criticality in the finite-size scaling (FSS) regime $L \ll \xi(\beta)$, where L is the sample size and $\xi(\beta)$ the second-moment correlation length at inverse temperature β . Here we will consider its scaling properties in the Thermodynamic limit (ThL) regime $L \gg \xi(\beta)$ where the properties of a finite-size sample if normalized correctly are independent of L and so are the same as those of the infinite-size model. (A standard rule of thumb for the onset of the ThL regime is $L > 7\xi(\beta, L)$).

In Ising ferromagnets, the second field derivative of the susceptibility χ_4 in a hypercubic lattice is directly related to the Binder cumulant, see Eq. 10.2 of Ref. [2], through

$$2g(\beta, L) = \frac{-\chi_4}{L^d \chi^2} = \frac{3\langle m^2 \rangle^2 - \langle m^4 \rangle}{\langle m^2 \rangle^2} \quad (1)$$

The susceptibility χ scales with the critical exponent γ , and the critical exponent for the second field derivative of the susceptibility χ_4 (also called the non-linear susceptibility), is [3]

$$\gamma_4 = \gamma + 2\Delta_{\text{gap}} = d\nu + 2\gamma \quad (2)$$

because of very basic RGT scaling and hyperscaling [4] relationships between exponents. ν and γ are the standard critical exponents for the correlation length and the susceptibility; a textbook definition of hyperscaling is : "Identities obtained from the generalised homogeneity assumption involve the space dimension d , and are known as hyperscaling relations." [5]. Explicitly quoting Ref. [6] : "Below the upper critical dimension, the following hyperscaling relations are supposed to be valid:

$2 - \alpha = d\nu$, and $2\Delta_{\text{gap}} = d\nu + \gamma$ where Δ_{gap} is the gap exponent, which controls the radius of the disk in the complex-temperature plane without zeroes, i.e. the gap, of the partition function (Yang-Lee theorem)".

Thus in the ThL regime the normalized Binder cumulant $L^d g(\beta, L)$ (or alternatively $\chi_4(\beta)/(2\chi(\beta)^2)$) scales with the critical exponent $(d\nu + 2\gamma) - 2\gamma = d\nu$, together with correction terms as for any such observable.

For high temperatures, it can be noted that in any $S = \frac{1}{2}$ Ising system the infinite-temperature (i.e. independent spins) limit for the Binder cumulant is $g(0, N) \equiv 1/N$, where N is the number of spins; $N = L^d$ for a hypercubic lattice so at infinite temperature $L^d g(\beta, L) \equiv 1$.

Hyperscaling is well established in standard models, such as the Ising models in dimensions less than the upper critical dimension, but many years ago hyperscaling relations were predicted to break down in quenched random systems [7]. Two hyperscaling relations have been quoted above; the first is well known and concerns the specific heat exponent α . The breakdown of this hyperscaling relation in the Random Field Ising model has been extensively studied [8, 9]. In the Ising spin glasses which we discuss below α is strongly negative and so is very hard to measure directly; we will be concerned only with the second hyperscaling relation which is less well known. We are aware of no tests of this hyperscaling relation in a system with quenched randomness such as a spin glass.

First we outline the general scaling approach, which follows Ref. [10]. The Wegner scaling expression [11] for an observable $Q(\tau)$ in the ThL regime is

$$Q(\tau) = C_Q \tau^{-\lambda} (1 + a_Q \tau^\theta + \dots) \quad (3)$$

where τ is a temperature scaling variable which tends to zero at criticality $\beta = \beta_c$; $Q(\tau)$ diverges with the critical exponent λ . In order to cover the entire paramagnetic temperature range, the conventional RGT scaling variable $t = (T - T_c)/T_c$ cannot be used as the temperature scaling variable because it diverges at infinite temperature. Following Wegner and High Temperature Scaling Expansion (HTSE) studies [3, 12] it is appropriate to use for Ising models the alternative temperature variable $\tau = 1 - \beta/\beta_c$, which tends to 1 at infinite tem-

perature. For Ising spin glasses (ISGs) having an interaction distribution with symmetry between positive and negative interactions, an appropriate scaling variable is $\tau = 1 - (\beta/\beta_c)^2$ [10, 13]. It is convenient to normalise all observables $Q(\tau)$ in such a way that the infinite temperature limit is 1, not 0 or ∞ , as otherwise a diverging set of correction terms would be required. The observables $\chi(\tau, L)$ and $L^d g(\tau, L)$ automatically obey this condition. The second moment correlation length $\xi(\tau, L)$ fulfills the condition when normalized to $\xi(\tau, L)/\beta^{1/2}$ in Ising models and to $\xi(\tau, L)/\beta$ in ISGs [10]. As will be seen below, with this approach data can be fitted to high precision over the entire paramagnetic temperature range from criticality to infinity with a minimal set of Wegner correction terms (in principle there is an infinite set of correction terms but with these normalisations the higher order terms become extremely weak). Assuming β_c is known or can be estimated precisely, the true critical exponents for the various observables can be estimated quite accurately from ThL data without the need to approach β_c closely.

II. ISING MODELS

We will first study two canonical Ising models: the square lattice model in dimension 2 and the simple cubic model in dimension 3, in order to validate our method for testing hyperscaling. We will choose as the thermal scaling variable in the Ising models $\tau = 1 - \beta/\beta_c$. β_c is known exactly in dimension 2 and to very high precision in dimension 3 [14]. For the simulation data the standard finite L definition for the second moment correlation length $\xi(\beta, L)$ through the Fourier transformation of the correlation function has been used, see Ref. [15], Eq. 14. We will follow the "extended scaling" convention introduced above and take the normalized correlation length, $\xi(\beta, L)/\beta^{1/2}$. The ThL normalized correlation length behaves as

$$\frac{\xi(\beta, L)}{\beta^{1/2}} = C_\xi \tau^{-\nu} (1 + a_\xi \tau^\theta + \dots) \quad (4)$$

It diverges with the standard critical exponent ν at criticality, and tends to 1 exactly at infinite temperature $\tau = 1$ for any dimension d . The term in τ^θ is the leading Wegner correction [11]. With the approach we follow, as ThL correlation length corrections are relatively small for these Ising models in either dimension 2 or dimension 3 [16, 17] the effective correlation length exponent $\nu(\tau) = \partial \ln[\xi(\beta, L)/\beta^{1/2}]/\partial \ln \tau$ is only weakly temperature dependent from criticality to close to infinite temperature. It is not necessary to go very close to criticality in order to observe an effective exponent $\nu(\tau)$ very similar in value to the true critical value. When simulation data for different sizes L are displayed together the ThL regime can be identified by inspection as the regime where the observable becomes L independent. A very detailed analysis of susceptibility, correlation length and

specific heat data for the 3D Ising model following the present approach is given in Ref. [16].

Now consider the Binder cumulant in the Ising models. From the relations above, the normalized ThL Binder cumulant $L^d g(\tau, L)$ has an infinite-temperature limit which is strictly 1, and a ThL regime behavior with a critical exponent $d\nu$ if hyperscaling holds, together with Wegner corrections as for other observables, so:

$$L^d g(\tau, L) \tau^{d\nu} = C_g (1 + a_g \tau^\theta + \dots) \quad (5)$$

Once again if the correction terms are relatively weak an approximately asymptotic behavior, with an effective exponent very similar to $d\nu$, will set in well before true criticality.

There is a hyperuniversal combination of critical amplitudes, the "dimensionless renormalized coupling constant" [3], which with the present conventions then can be written as $G_r = \beta_c^{d/2} C_g / C_\xi^d$.

So, in an Ising model if we plot the logarithm of the normalized Binder cumulant $y(\tau) = \ln[L^d g(\tau, L)]$ and the logarithm of the normalized correlation length $y(\tau) = \ln[\xi(\tau, L)/\beta^{1/2}]$ against $x = \ln \tau$, the ThL negative slopes $\partial y(\tau)/\partial \ln \tau$ will tend to $d\nu$ and ν respectively as criticality is approached; for all L the data will tend to $y(\tau) = 0$ at the infinite temperature $\tau = 1$ limit.

For the Ising model ferromagnets on the 2D square lattice and the 3D simple cubic lattice, data are displayed in this way in Figs. 1 and 2 respectively. The ThL envelope where data become independent of L for large enough L can be identified by inspection.

Data for these plots are taken from numerical simulations for the 2D square lattice Ising model, for sample sizes $L = 6, 12, 24$, and 32 , and in the 3D data from numerical simulations simple cubic Ising ferromagnet [14] for sample sizes $L = 8, 12, 16$, and 24 . The ThL simulation curves agree in full detail with data obtained by explicitly summing tabulated HTSE series [3, 12, 18].

For these two Ising models all the relevant ThL parameters including the critical exponents $\nu \equiv 1$ and $\nu = 0.6300$ respectively and the critical amplitudes, are already known [3, 12, 19]. For the 2D Ising model with the HTSE parameters, assuming hyperscaling, and keeping only the leading correction terms with analytic correction term exponents $\theta = 1$, the calculated curves with no free parameters are

$$\frac{\xi(\tau)}{\beta^{1/2}} = 0.854\tau^{-1} (1 + 0.171\tau) \quad (6)$$

$$\frac{\chi_4(\tau)}{2\chi(\tau)^2} = 2.365\tau^{-2} (1 + 0.577\tau) \quad (7)$$

which are in excellent agreement with the ThL simulation data envelope, (where $L^2 g(\tau, L)$ replaces $\chi_4(\tau)/(2\chi(\tau)^2)$).

For the 3D Ising model we again take the known critical temperature and critical amplitudes. While the effective leading correction term exponent for the correlation length takes the standard value for this model,

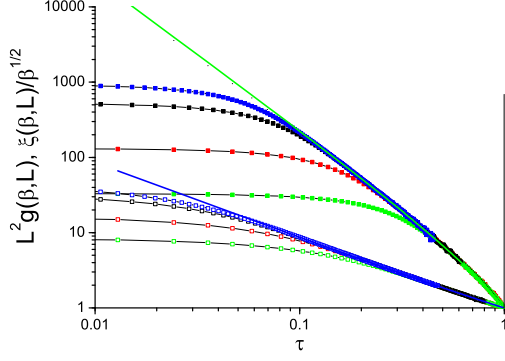


FIG. 1. (Color on line) The 2D ferromagnetic Ising model. Upper data sets $\ln[L^2 g(\beta, L)]$ against τ , lower data sets $\ln[\xi(\beta, L)/\beta^{1/2}]$ against $\ln \tau$ where $g(\beta, L)$ is the Binder cumulant and $\xi(\beta, L)$ is the second-moment correlation length. Sizes $L = 32, 24, 12, 6$, top to bottom. Smooth (upper) green curve and (lower) blue curve: fits (see text).

$\theta = 0.52$ [17], the optimal fit corresponds to an effective θ_{eff} for the HTSE χ_4 data, and hence for $L^3 g(\tau, L)$, of $\theta_{\text{eff}} \approx 1.4$. This can be ascribed for instance to the presence of a strong higher order correction term with exponent $1 + \theta$ [20]. The simulation data and the essentially exact HTSE data (see Ref. [3], Fig. 19) can be fitted with the same large effective exponent as the simulation data. The HTSE curves calculated with the parameters

$$\frac{\xi(\tau)}{\beta^{1/2}} = 1.074\tau - 0.63(1 - 0.069\tau^{0.52}) \quad (8)$$

$$\frac{\chi_4(\tau)}{2\chi(\tau)^2} = 1.523\tau - 1.89(1 - 0.343\tau^{1.5}) \quad (9)$$

are in excellent agreement with the simulation ThL envelope data (with $L^3 g(\tau, L)$ replacing $\chi_4(\tau)/(2\chi(\tau)^2)$).

The 3D ThL critical $L \equiv \infty, \tau \rightarrow 0$ limit for the dimensionless renormalisation constant $G_r = \beta_c^{d/2} C_g / C_\xi^d$ is 1.226, which is quite different from the finite size scaling $\tau \equiv 0, L \rightarrow \infty$ limit for the same ratio which is 0.2803.

In both models, over the entire temperature range covered by the simulation data (excepting the region close to infinite temperature), the almost asymptotic ratio of the $L^d g(\tau, L)$ and $\xi(\tau, L)/\beta^{1/2}$ log-log slopes is very close to d , verifying that the hyperscaling rule is respected and incidentally validating once again the utility of the extended scaling normalization of the correlation length for Ising ferromagnet analyses over wide temperature ranges [16, 21]. (A “cross-over” behavior of high temperature data in Ising ferromagnets [22] is an artefact [23]).

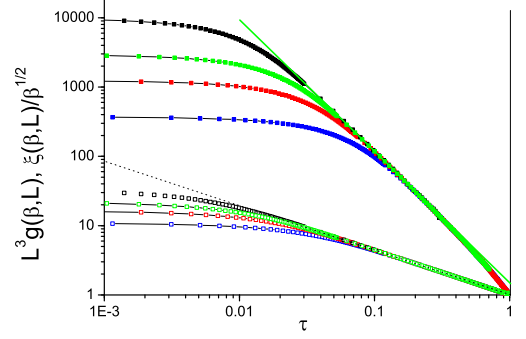


FIG. 2. (Color on line) The 3D ferromagnetic Ising model. Upper data sets $\ln[L^3 g(\beta, L)]$ against $\ln \tau$, lower data sets $\ln[\xi(\beta, L)/\beta^{1/2}]$ against τ where $g(\beta, L)$ is the Binder cumulant and $\xi(\beta, L)$ is the second-moment correlation length. Sizes $L = 24, 16, 12, 8$, top to bottom. Smooth (upper) green curve and (lower) dashed curve: fits (see text)

III. ISING SPIN GLASSES

Now we turn to ISGs. The standard ISG Hamiltonian is $\mathcal{H} = -\sum_{ij} J_{ij} S_i S_j$ with the near neighbor symmetric distributions normalized to $\langle J_{ij}^2 \rangle = 1$. The normalized inverse temperature is $\beta = (\langle J_{ij}^2 \rangle / T^2)^{1/2}$. The Ising spins live on simple hyper-cubic lattices with periodic boundary conditions. The spin overlap parameter is defined as usual by

$$q = \frac{1}{L^d} \sum_i S_i^A S_i^B \quad (10)$$

where A and B indicate two copies of the same system. Klein *et al* [24] quote exactly the same hyperscaling relation Eq. (2) for χ_4 in the ISGs as in the Ising ferromagnets (with the spin overlap moments $\langle q^2 \rangle$ and $\langle q^4 \rangle$ replacing the magnetization moments $\langle m^2 \rangle$ and $\langle m^4 \rangle$), so the RGT prediction for the ISG Binder cumulant critical exponent is again $\gamma_4 - 2\gamma = d\nu$. Because the interaction parameter in the ISGs is $\langle J_{ij}^2 \rangle$ the appropriate ISG scaling variable is $\tau = 1 - (\beta/\beta_c)^2$ [10, 13] and the appropriate normalized correlation length is $\xi(\tau, L)/\beta$ [10].

The simulation data in the ISGs are the same as those in Refs. [25, 26] where the simulation techniques have already been described in detail. Means were taken on at least 8192 samples for each L with of the order of 40 different temperatures. The maximum sizes studied were $L = 24$ for the bimodal model and $L = 16$ for the Gaussian model in dimension 3, $L = 14$ for the bimodal model, $L = 12$ for the Gaussian and Laplacian models in dimension 4 and $L = 10$ in dimension 5. Particular attention was paid to achieving full equilibration; here we are only concerned with data in the ThL above the ordering temperature where equilibration is reached much faster than at or below the ordering temperature, so one

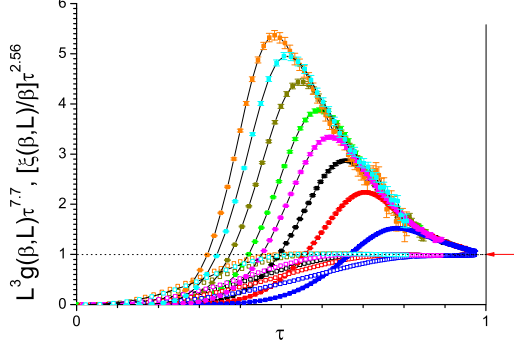


FIG. 3. (Color on line) The 3D bimodal ISG model. Upper data sets $L^3 g(\beta, L) \tau^{7.7}$ against τ , lower data sets $[\xi(\beta, L)/\beta] \tau^{2.56}$ against τ where $g(\beta, L)$ is the Binder cumulant and $\xi(\beta, L)$ is the second-moment correlation length. Sizes $L = 24, 20, 16, 12, 10, 8, 6, 4$ (upper set) and $L = 24, 20, 12, 6$ (lower set), top to bottom.

can have full confidence that the samples were in equilibrium for the temperature range of interest here. For the 3D bimodal model a comparison with tabulated data generously provided as a supplement to Ref. [15] confirms equilibration.

We first display the data for the 3D bimodal and Gaussian ISG models in a form which provides a preliminary qualitative test of the hyperscaling rule, see Figs. 3 and 4. We take the most recent estimations for the critical parameters from the literature: $\beta_c = 0.909$ and $\nu = 2.56$ for the bimodal model [27], $\beta_c = 1.05$ and $\nu = 2.44$ for the Gaussian model [28]. For each model we then plot together on the same figure the products $[\xi(\tau, L)/\beta] \tau^\nu$ and $L^d g(\tau, L) \tau^{d\nu}$ against τ . If hyperscaling is respected, we would expect that in each case both sets of ThL envelope curves should lie close to 1 for the whole range of τ , to within weak correction terms. For both models the $[\xi(\tau, L)/\beta] \tau^\nu$ ThL envelope curves indeed take this form, but the $L^d g(\tau, L) \tau^{d\nu}$ ThL envelope curves (on the right hand side of the observed peaks in the figures) behave in a totally different manner suggestive of divergence with increasing L . This is a dramatic qualitative demonstration that at least for these two ISG models the hyperscaling rule is not obeyed.

To obtain quantitative information, we will follow up by presenting these ISG data in just the same way as in the figures for the Ising models. Figs. 5 and 6 show log-log plots of $L^3 g(\tau, L)$ against τ (upper data sets) and $\xi(\tau, L)/\beta$ against τ (lower data sets) for the 3D bimodal ISG and the 3D Gaussian ISG. We have assumed again for the bimodal model $\beta_c = 0.909$ [27] and for the Gaussian model $\beta_c = 1.05$ [28]. The finite size scaling correction exponent for the bimodal model has been estimated to be $\omega \approx 1.1$ [15, 27] which corresponds to a Wegner correction exponent $\theta = \nu\omega \approx 2.5$. There is no equivalent estimate available for the Gaussian model so we will

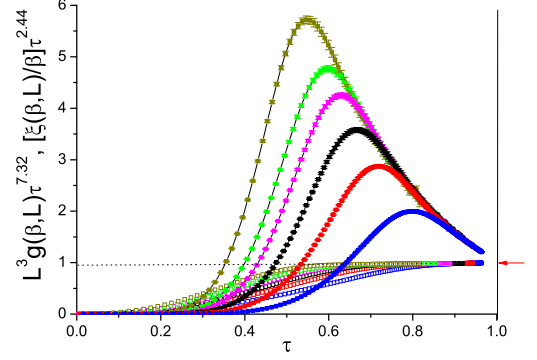


FIG. 4. (Color on line) The 3D Gaussian ISG model. Upper data sets $L^3 g(\beta, L) \tau^{7.2}$ against τ , lower data sets $[\xi(\beta, L)/\beta] \tau^{2.44}$ against τ where $g(\beta, L)$ is the Binder cumulant and $\xi(\beta, L)$ is the second-moment correlation length. Sizes $L = 16, 12, 10, 8, 6, 4$ (both sets), top to bottom.

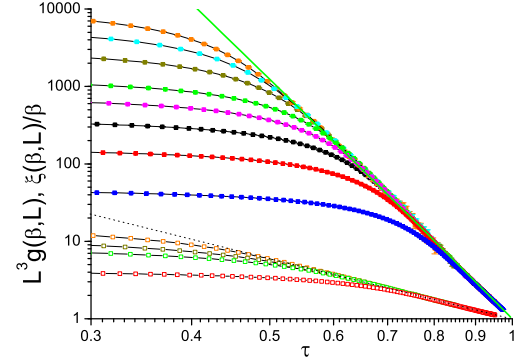


FIG. 5. (Color on line) The 3D bimodal ISG model. Upper data sets $\ln[L^3 g(\beta, L)]$ against $\ln \tau$, lower data sets $\ln[\xi(\beta, L)/\beta]$ against $\ln \tau$ where $g(\beta, L)$ is the Binder cumulant and $\xi(\beta, L)$ is the second-moment correlation length. Sizes $L = 24, 20, 16, 12, 10, 8, 6, 4$ (upper set) and $L = 24, 20, 12, 6$ (lower set), top to bottom. Smooth (upper) green curve and (lower) dashed curve: fits (see text)

assume the same effective θ .

Fits to the $\xi(\tau, L)/\beta$ ThL envelopes give effective exponents $\nu = 2.5(1)$ for the bimodal ISG and $\nu = 2.4(1)$ for the Gaussian ISG with negligible correction terms. These estimates, from intermediate and high temperature data, are very similar to the critical values quoted above estimated by finite size scaling, showing that corrections to scaling are playing only a very minor role over the whole paramagnetic temperature range. The fits for the $L^3 g(\tau, L)$ ThL envelopes are $1.2\tau^{-10.05}(1 - 0.17\tau^{2.5})$ for the bimodal model and $2.0\tau^{-9.5}(1 - 0.50\tau^{2.5})$ for the Gaussian model, i.e. critical exponent estimates which are $4.00(5)\nu$ and $3.96(5)\nu$ respectively, so well above the hyperscaling value of 3ν .

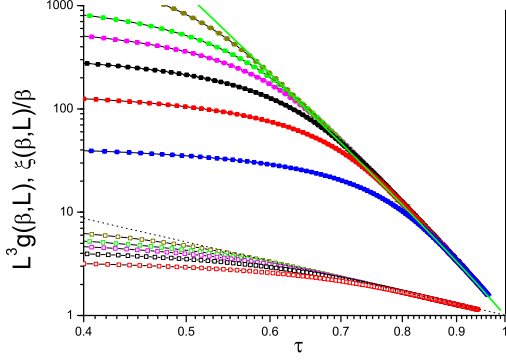


FIG. 6. (Color on line) The 3D Gaussian ISG model. Upper data sets $\ln[L^3 g(\beta, L)]$ against $\ln \tau$, lower data sets $\ln[\xi(\beta, L)/\beta]$ against $\ln \tau$ where $g(\beta, L)$ is the Binder cumulant and $\xi(\beta, L)$ is the second-moment correlation length. Sizes $L = 16, 12, 10, 8, 6, 4$ (upper set) and $L = 16, 12, 10, 8, 6$ (lower set), top to bottom. Smooth (upper) green curve and (lower) dashed curve: fits (see text)

Continuing on to dimension 4, Figures 7, 8 and 9 show data presented in the same manner, for the bimodal, Gaussian and Laplacian 4D ISG models. The critical inverse temperatures are $\beta_c = 0.505$ for the bimodal model [25], $\beta_c = 0.555$ for the Gaussian model [25, 29] and $\beta_c = 0.419$ for the Laplacian model [30]. Fits to the ThL envelopes give effective exponents $\nu = 1.10$ for the bimodal, $\nu = 1.02$ for the Gaussian and $\nu = 0.95$ for the Laplacian model. These estimates from intermediate and high temperature data are very similar to the critical values estimated by finite size scaling, $\nu = 1.12$, $\nu = 1.02$ [25] and $\nu = 0.99$ [30] respectively showing that corrections to scaling at temperatures well above T_c are again playing only a very minor role. The fit to the ThL envelope of the bimodal $L^4 g(\tau, L)$ data set is $L^4 g(\tau, L) = 0.22\tau^{-5.5}(1 + 3.5\tau^{2.0})$ so with a very strong correction to scaling. The fit to the Gaussian ThL envelope is $L^4 g(\tau, L) = 0.9\tau^{-4.5}(1 + 0.1\tau^{1.5})$ and the fit to the Laplacian ThL envelope is $L^4 g(\tau, L) = 1.2\tau^{-4.6}(1 - 0.17\tau^{1.5})$ so both with rather weak corrections to scaling. The $L^4 g(\tau, L)$ critical exponent estimates are $5.0(1)\nu$, $4.4(1)\nu$ and $4.65(10)\nu$ respectively so well above the hyperscaling prediction, for which the values should be equal to 4ν .

Finally in dimension 5 the bimodal and Gaussian ISG inverse critical temperatures are $\beta_c = 0.3885$ and $\beta_c = 0.419$ [30]. The same procedure is followed as for the other dimensions, Figures 10 and 11.

Fits to the $\xi(\tau, L)/\beta$ ThL envelopes give effective exponents $\nu = 0.75(1)$ for the 5D bimodal ISG and $\nu = 0.76(1)$ for the 5D Gaussian ISG with negligible correction terms. These estimates, from intermediate and high temperature data, are similar to the critical values estimated by finite size scaling, $\nu = 0.77(2)$, $\nu = 0.72(1)$ respectively [30], showing that corrections to scaling are playing only a minor role over the whole paramagnetic

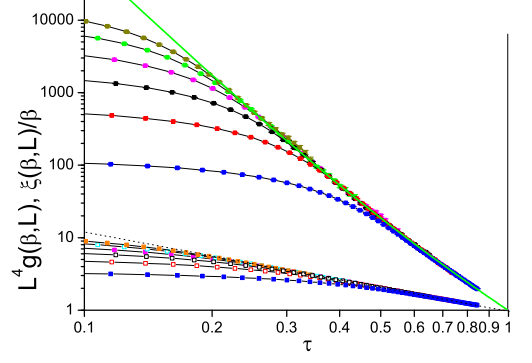


FIG. 7. (Color on line) The 4D bimodal ISG model. Upper data sets $\ln[L^4 g(\beta, L)]$ against $\ln \tau$, lower data sets $\ln[\xi(\beta, L)/\beta]$ against $\ln \tau$ where $g(\beta, L)$ is the Binder cumulant and $\xi(\beta, L)$ is the second-moment correlation length. Sizes $L = 14, 12, 10, 8, 6, 4$ (both sets), top to bottom. Smooth (upper) green curve and (lower) dashed curve: fits (see text)

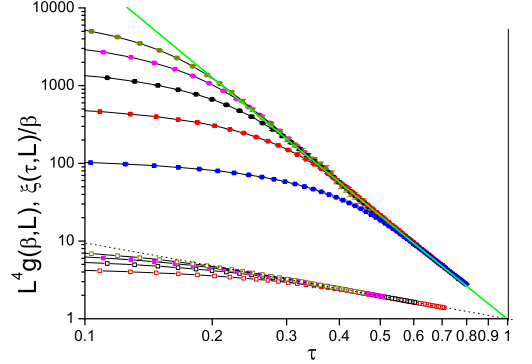


FIG. 8. (Color on line) The 4D Gaussian ISG model. Upper data sets $\ln[L^4 g(\beta, L)]$ against $\ln \tau$, lower data sets $\ln[\xi(\beta, L)/\beta]$ against $\ln \tau$ where $g(\beta, L)$ is the Binder cumulant and $\xi(\beta, L)$ is the second-moment correlation length. Sizes $L = 12, 10, 8, 6, 4$ (upper set) and $L = 12, 10, 8, 6$ (lower set), top to bottom. Smooth (upper) green curve and (lower) dashed curve: fits (see text)

temperature range for this observable. The fits for the $L^5 g(\tau, L)$ ThL envelopes are $0.20\tau^{-4.1}(1 + 4.0\tau^{1.7})$ for the bimodal model and $0.50\tau^{-3.6}(1 + 1.0\tau^{1.0})$ for the Gaussian model, i.e. critical exponent estimates which are $5.4(2)\nu$ and $4.9(2)\nu$ respectively. The corrections to scaling are very strong and the correction exponents θ_{eff} are not accurately determined so the uncertainties are stronger than for 3D and 4D ; for 5D the data indicate an exponent ratio which is compatible with or weakly above the hyperscaling value of 5ν .

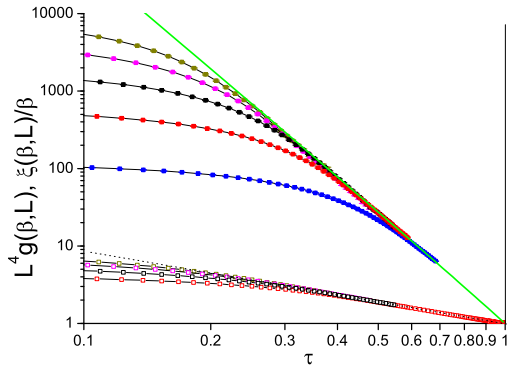


FIG. 9. (Color on line) The 4D Laplacian ISG model. Upper data sets $\ln[L^4 g(\beta, L)]$ against $\ln \tau$, lower data sets $\ln[\xi(\beta, L)/\beta]$ against $\ln \tau$ where $g(\beta, L)$ is the Binder cumulant and $\xi(\beta, L)$ is the second-moment correlation length. Sizes $L = 12, 10, 8, 6, 4$ (upper set) and $L = 12, 10, 8, 6$ (lower set), top to bottom. Smooth (upper) green curve and (lower) dashed curve: fits (see text)

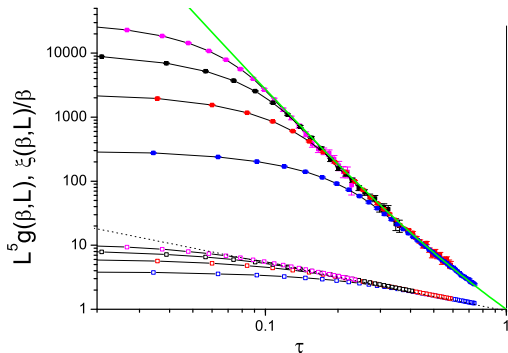


FIG. 10. (Color on line) The 5D bimodal ISG model. Upper data sets $\ln[L^5 g(\beta, L)]$ against $\ln \tau$, lower data sets $\ln[\xi(\beta, L)/\beta]$ against $\ln \tau$ where $g(\beta, L)$ is the Binder cumulant and $\xi(\beta, L)$ is the second-moment correlation length. Sizes $L = 10, 8, 6, 4$, top to bottom in each set. Smooth (upper) green curve and (lower) dashed curve: fits (see text)

IV. CONCLUSION

From RGT, the critical exponent for the normalised Binder cumulant in dimension d , $\chi_4(\tau, L)/(2\chi(\tau, L)^2) = L^d g(\tau, L)$ should be strictly equal to $d\nu$ in all models below the upper critical dimension. However, the scaling relation is based on the assumption that the standard Josephson hyperscaling rule Eq. 2 holds. The derivation leading to this rule assumes translational invariance (see [7, 31]). It is well established that in the Random Field Ising model (RFIM), which is not translationally invariant, the hyperscaling rule $2 - \alpha = \beta + 2\gamma = \nu d$ is replaced by $2 - \alpha = \beta + 2\gamma = \nu(d - \theta)$; here θ is a hyperscaling vi-

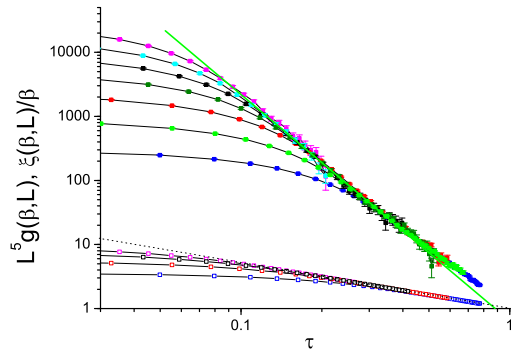


FIG. 11. (Color on line) The 5D Gaussian ISG model. Upper data sets $\ln[L^5 g(\beta, L)]$ against $\ln \tau$, lower data sets $\ln[\xi(\beta, L)/\beta]$ against $\ln \tau$ where $g(\beta, L)$ is the Binder cumulant and $\xi(\beta, L)$ is the second-moment correlation length. Sizes $L = 10, 9, 8, 7, 6, 5, 4$ (upper set) and $L = 10, 8, 6, 4$ (lower set), top to bottom. Smooth (upper) green curve and (lower) dashed curve: fits (see text)

olation exponent (not to be confused with the correction exponent) and it is believed that $\theta = \gamma/\nu$ (two exponent scaling) in the RFIM [8, 9]. ISGs are not translationally invariant either. In ISGs α is always negative and very large, and so is very hard to estimate directly. The ISG Binder cumulant scaling behavior reported here provides another test of hyperscaling, for a Binder cumulant hyperscaling relation on seven different ISG models.

We conclude empirically from the simulation data that the basic RGT scaling law with the second Josephson hyperscaling rule does not hold in ISGs, at least in dimensions 3 and 4, with dimension 5 being uncertain. It may be relevant that for spin glasses the situation concerning the gap exponent Δ_{gap} referred to above is more complicated than for ferromagnets, or even for diluted ferromagnets, as the locations of Yang-Lee zeros are not restricted to the imaginary-field axis [32].

It has been generally accepted that RGT implies that in ISGs critical exponents and the values of dimensionless parameters at criticality should be universal, whatever the form of the interaction distribution. It may be relevant that numerically this RGT universality rule also has been found not to hold, for ISGs in 4D [25, 26], 2D [33] and 5D [30]. However, in the RFIM universality has been shown to hold [34]. The link between non-universality and hyperscaling breakdown is not clear to us. However it appears that none of the standard RGT rules should be taken for granted in ISGs.

It has been authoritatively stated that “classical tools of RGT analysis are not suitable for spin glasses” [35–37]. The numerical results taken together indeed appear to be a clear empirical indication that a fundamentally novel theoretical approach is required for scaling at spin glass transitions.

ACKNOWLEDGMENTS

We would like to thank Professor A. Aharony, Dr. P. Butera and Dr. C. Müller for helpful comments.

The computations were performed on resources provided by the Swedish National Infrastructure for Computing (SNIC) at the High Performance Computing Center North (HPC2N) and Chalmers Centre for Computational Science and Engineering (C3SE).

-
- [1] K. Binder, Z. Physik B **43**, 119 (1981); Phys. Rev. Lett. **47**, 693 (1981).
 - [2] V. Privman, P. C. Hohenberg and A. Aharony, "Universal Critical-Point Amplitude Relations", in "Phase Transitions and Critical Phenomena" (Academic, NY, 1991), eds. C. Domb and J.L. Lebowitz, **14**, 1.
 - [3] P. Butera and M. Comi, Phys. Rev. B **65**, 144431 (2002).
 - [4] B. D. Josephson, Phys. Lett. **21**, 608 (1966).
 - [5] B. Simons, Phase Transitions and Collective Phenomena, Cambridge University Press (1997).
 - [6] A. Pelissetto and E. Vicari, Phys. Rept. **368**, 549 (2002), arXiv:0012164.
 - [7] M. Schwartz, Europhys.Lett. **15**, 777 (1991).
 - [8] R. L. C. Vink, T. Fischer, and K. Binder, Phys. Rev. E **82**, 051134 (2010).
 - [9] M. Gofman, J. Adler, A. Aharony, A. B. Harris, and M. Schwartz, Phys. Rev. Lett. **71**, 1569 (1993).
 - [10] I. A. Campbell, K. Hukushima, and H. Takayama, Phys. Rev. Lett. **97**, 117202 (2006).
 - [11] F. J. Wegner, Phys. Rev. B **5**, 4529 (1972).
 - [12] P. Butera, M. Comi and A. J. Guttmann, Phys. Rev. B **67**, 054402 (2003).
 - [13] D. Daboul, I. Chang, and A. Aharony, Eur. Phys. J. B **41**, 231 (2004).
 - [14] R. Häggkvist, A. Rosengren, P. H. Lundow, K. Markström, D. Andrén, and P. Kundrotas, (2007), Adv. Phys. **56**, 653 (2007).
 - [15] M. Hasenbusch, A. Pelissetto and E. Vicari, Phys. Rev. B **78**, 214205 (2008).
 - [16] I. A. Campbell and P. H. Lundow, Phys. Rev. B **83**, 014411 (2011).
 - [17] I. A. Campbell and P. Butera, Phys. Rev. B **78**, 024435 (2008).
 - [18] P. Butera and M. Comi, J. Stat. Phys. **109**, 311 (2002).
 - [19] D. Simmons-Duffin, JHEP **06**, 1 (2015).
 - [20] P. Butera, private communication.
 - [21] I.A. Campbell and P. Butera, Phys. Rev. B **78**, 024435 (2008).
 - [22] E. Luijten, H. W. J. Blöte, and K. Binder, Phys. Rev. Lett. **79**, 561 (1997).
 - [23] P. H. Lundow and I. A. Campbell, Phys. Rev. B **83**, 184408 (2011).
 - [24] L. Klein, J. Adler, A. Aharony, A. B. Harris and Y. Meir, Phys. Rev. B **43**, 11249 (1991).
 - [25] P. H. Lundow and I. A. Campbell, Phys. Rev.E **91**, 042121 (2015).
 - [26] P. H. Lundow and I. A. Campbell, Physica A **434**, 181 (2015).
 - [27] M. Baity-Jesi *et al* Phys. Rev. B **88**, 224416 (2013).
 - [28] H. G. Katzgraber, M. Körner, and A. P. Young, Phys.Rev.B **73**, 224432 (2006).
 - [29] T. Jörg and H. G. Katzgraber, Phys. Rev. B **77**, 214426 (2008).
 - [30] P. H. Lundow and I. A. Campbell, unpublished manuscript.
 - [31] C. A. Müller, Phys. Rev. A **91**, 023602 (2015).
 - [32] Y. Matsuda, M. Müller, H. Nishimori, T. Obuchi and A. Scardicchio, J. Phys. A: Math. Theor. **43**, 285002 (2010).
 - [33] P. H. Lundow and I. A. Campbell, Phys. Rev. E **93**, 022119 (2016).
 - [34] N. Fytas and V. Martin-Mayor, Phys. Rev. Lett. **110**, 227201 (2013).
 - [35] G. Parisi, R. Petronzio, and F. Rosati, Eur. Phys. J. B **21**, 605 (2001).
 - [36] M. Castellana, Eur. Phys. Lett. **95**, 47014 (2011).
 - [37] M. C. Angelini, G. Parisi, and F. Ricci-Tersenghi, Phys. Rev. B **87**, 134201 (2013).